**NEURAL REGENERATION RESEARCH**
November 2015, Volume 10, Issue 11
www.nrronline.org

RESEARCH ARTICLE

# MicroRNAs: a novel promising therapeutic target for cerebral ischemia/reperfusion injury?

**Xiao-li Min[1, 2], Ting-yong Wang[3], Yi Cao[4], Jia Liu[1], Jin-tao Li[1, #], Ting-hua Wang[1, *, #]**

1 Institute of Neuroscience, Kunming Medical University, Kunming, Yunnan Province, China
2 Faculty of Clinical Medicine, Yunnan University of Traditional Chinese Medicine; the First Affiliated Hospital of Yunnan University of Traditional Chinese Medicine, Kunming, Yunnan Province, China
3 School of Economics of Sichuan University, Chengdu, Sichuan Province, China
4 Department of Neurosurgery, the Second Affiliated Hospital of Kunming Medical University, Kunming, Yunnan Province, China

***Correspondence to:**
*Ting-hua Wang, M.D., Ph.D., tinghua_neuron@263.net.*

*# These authors contributed equally to this work.*

***orcid:***
*0000-0002-5353-4810 (Ting-hua Wang)*

***doi:** 10.4103/1673-5374.170302*
***http:**//www.nrronline.org/*

***Accepted:** 2015-07-10*

## Abstract

To determine the molecular mechanism of cerebral ischemia/reperfusion injury, we examined the microRNA (miRNA) expression profile in rat cortex after focal cerebral ischemia/reperfusion injury using miRNA microarrays and bioinformatic tools to systematically analyze Gene Ontology (GO) function classifications, as well as the signaling pathways of genes targeted by these differentially expressed miRNAs. Our results show significantly changed miRNA expression profiles in the reperfusion period after focal cerebral ischemia, with a total of 15 miRNAs up-regulated and 44 miRNAs down-regulated. Target genes of these differentially expressed miRNAs were mainly involved in metabolic and cellular processes, which were identified as hub nodes of a miRNA-GO-network. The most correlated pathways included D-glutamine and D-glutamate metabolism, the renin-angiotensin system, peroxisomes, the PPAR signaling pathway, SNARE interactions in vesicular transport, and the calcium signaling pathway. Our study suggests that miRNAs play an important role in the pathological process of cerebral ischemia/reperfusion injury. Understanding miRNA expression and function may shed light on the molecular mechanism of cerebral ischemia/reperfusion injury.

***Key Words:** nerve regeneration; microRNA; therapeutic target; cerebral ischemia/reperfusion injury; miRNA expression profiles; bioinformatics analysis; Gene Ontology analysis; molecular mechanism; KEGG pathway; neural regeneration*

***Funding:** This work was supported by grants from the National Natural Science Foundation of China, No. 81271358; Yunnan Science Foundation of China, No. 2013FZ199.*

*Min XL, Wang TY, Cao Y, Liu J, Li JT, Wang TH (2015) MicroRNAs: a novel promising therapeutic target for cerebral ischemia/reperfusion injury? Neural Regen Res 10(11):1799-1808.*

## Introduction

The main therapeutic methods for ischemic stroke ensure recanalization to restore blood flow and obtain reperfusion (Wechsler, 2011). But reperfusion itself can cause additional and unexpected brain damage, termed cerebral ischemia/reperfusion injury (Yellon and Hausenloy, 2007), which results in secondary energy failure and delayed cell death. There is strong evidence supporting this pathological process in studies involving gerbil (Arai et al., 1986) and rat (Lust et al., 2002) models, and even human patients (Horn and Schlote, 1992). The pathophysiological mechanisms of cerebral ischemia/reperfusion injury are complex, and include intracellular calcium overload, calcium sensitive proteinase activation, excitatory amino acid release, excessive generation of reactive oxygen species (ROS), lipid peroxidation (Wu et al., 2006), inflammation, and reduced mitochondrial respiratory function (Sims and Muyderman, 2010). MicroRNAs (miRNAs) have been implicated in the pathophysiological mechanisms of cerebral ischemia/reperfusion injury (Zhai et al., 2012; Huang et al., 2015). However, little is known about the bioinformatics of miRNA genomics involved in the molecular mechanisms of cerebral ischemia/reperfusion injury, and how these miRNAs exert their effects.

MiRNAs are small noncoding single-stranded RNA molecules with mature transcripts of 18 to 25 nucleotides long, which act as negative regulators of gene expression by binding to the 3′-untranslated region (UTR) of complementary or partially complementary target messenger RNAs (mRNAs), thereby downregulating target mRNAs *via* degradation or translational inhibition (Di et al., 2014). In the central nervous system, miRNAs have been correlated with modulation of multiple diseases and pathological processes, such as neurodegenerative disorders (Fagan and Perrin, 2012), cancers (Lages et al., 2012), stroke (Tan et al., 2009), and cerebral ischemia/ reperfusion injury (Zhai et al., 2012). Accordingly, miRNA expression profiles in animal models of cerebral ischemia/reperfusion injury are increasingly reported (Jeyaseelan et al., 2008; Dharap et al., 2009; Liu et al., 2010; Yuan et al., 2010). However, these studies have only demonstrated superficial changes in miRNAs (Lim et al., 2010; Zhai et al., 2012) or focus on the role of a single

miRNA in cerebral ischemia (Huang et al., 2015), and lack comprehensive analysis of their biological functions and downstream signaling transduction pathways.

In this study, we profiled miRNA expression following focal cerebral ischemia/reperfusion using microarray technology. Using bioinformatic tools, we systematically analyzed Gene Ontology (GO) function classifications as well as the signaling pathways of genes targeted by these differentially expressed miRNAs.

## Materials and Methods

### Animals and surgical procedures

Sixteen adult female Sprague-Dawley rats, weighing 200–240 g, were used for the experiments. They were purchased from Chengdu Dossy Experimental Animals Co., Ltd. (Chengdu, China), and maintained in a constant 12-hour dark/light cycle with standard laboratory chew and food-water available *ad libitum*. All experimental procedures were performed in accordance with the National Institute of Health Guide for the Care and Use of Labortory Animals (NIH Publication No. 85-23, revised 1996) and approved by the Animal Care and Use Ethics Committee of Kunming Medical University.

All animals were equally and randomly assigned to two groups: sham and cerebral ischemia/reperfusion injury (**Table 1**). Rats in the cerebral ischemia/reperfusion injury group were subjected to intraluminal occlusion of the right middle cerebral artery (MCAO), as described previously (Sun et al., 2012). A MCAO monofilament suture with a blunt tip (0.32 ± 0.02 mm in diameter, type 2432-A4) was purchased from Beijing Cinontech Co., Ltd. (Beijing, China). After 90 minutes of occlusion, the suture was removed to restore blood flow and allowed reperfusion until 72 hours. Rats in the sham group were subjected to suture insertion into the origin of the internal carotid artery, but not the middle cerebral artery, with the remaining procedures identical to those in the cerebral ischemia/reperfusion injury group. According to a previously described method (Longa et al., 1989), rat models were selected as follows: (1) Zea Longa scores ≥ 2; (2) no concurrent subarachnoid hemorrhage or cerebral hemorrhage; and (3) survival until the predetermined time point. During surgery, the core body temperature of rats was maintained at 37.0 ± 0.5°C using a heating lamp and an animal body temperature maintenance instrument (type YLS-20A; ZS Dichuang, Beijing, China). Three days after surgery, all rats were sacrificed and the entire brain rapidly removed and incubated with triphenyl tetrazolium chloride (TTC) (Beijing Cinontech Co., Ltd.) ($n$ = 5 rats in sham and cerebral ischemia/reperfusion injury groups, respectively), with the ipsilateral cerebral cortex harvested for miRNA microarray ($n$ = 3 rats in sham and cerebral ischemia/reperfusion injury groups, respectively).

### Triphenyl tetrazolium chloride (TTC) staining and quantitation of infarct volume

Whole brain tissue was harvested after 90 minutes of ischemia followed by 72 hours of reperfusion, ensuring that upon removal, the integrity of the brain was maintained. The brains were then placed in specific brain slice molds and rapidly frozen at −20°C for 20 minutes to enable easy slicing. Brain tissue between –2.00 mm and +4.00 mm from Bregma was cut into 2.0-mm-thick coronal slices. Brain slices were then incubated in 2% TTC solution at 37°C for 30 minutes, avoiding light with a foil cover as described before (Kam et al., 2011), and later photographed using a digital camera. Triphenyl tetrazolium chloride is slightly heat and light unstable, and can be enzymatically reduced by dehydrogenases rich in living tissue, which results in a red color. However, in necrotic tissue, TTC remains white due to lack of such enzymatic activity. Thus, the infarct region appears white, while non-ischemic regions are red.

The infarct volume was determined from digitized images using the ImageJ software package (National Institute of Health, USA). Infarction size and total area of the contralateral hemisphere were measured in all sections. To compensate for the effect of brain edema after cerebral infarction, the corrected infarct volume was calculated as the sum of the infarct areas multiplied by the section thickness (2.0 mm), and expressed as a percentage of the contralateral (non-occluded) hemisphere (Selvamani et al., 2012).

### Isolation of total RNA

In the cerebral ischemia/reperfusion injury group, peri-lesion tissue from the ipsilateral ischemic cortex was obtained from rats at 3 days after ischemia and reperfusion, with the corresponding cortex harvested from the sham group as well. Total RNA was extracted using TRIzol Reagent (Invitrogen, Carlsbad, CA, USA) and the miRNeasy mini kit (Qiagen, Germantown, MD, USA), according to the manufacturer's instructions, then dissolved in RNAase-free deionized water. Purity and integrity of total RNA was measured using a Nanodrop spectrophotometer (ND-1000, Thermo Fisher Scientific Inc., Waltham, MA, USA) and standard denaturing agarose gel electrophoresis.

### RNA labeling and miRNA microarray

After passing RNA quality measurement, total RNA samples were labeled using the miRCURY™ Hy3™/Hy5™ Power labeling kit (Exiqon, Vedbaek, Denmark), according to the manufacturer's guideline. One microgram of each sample was 3′-end-labeled with a Hy3™ fluorescent label using T4 RNA ligase and the following procedure: RNA in 2.0 μL water was combined with 1.0 μL CIP buffer and CIP (Exiqon). The mixture was incubated for 30 minutes at 37°C, then for 5 minutes at 95°C. Next, 3.0 μL labeling buffer, 1.5 μL fluorescent label (Hy3™), 2.0 μL DMSO, and 2.0 μL labeling enzyme were added to the mixture. The labeling reaction was incubated for 1 hour at 16°C and terminated by incubation for 15 minutes at 65°C.

Following labeling, Hy3™-labeled samples were hybridized to the miRCURY™ LNA Array (v.16.0) (Exiqon). According to the array manual, a total of 25 μL mixture from Hy3™-labeled samples and 25 μL hybridization buffer was first denatured for 2 minutes at 95°C, incubated on ice for

**Table 1 Animal groups for miRNA array analysis and triphenyl tetrazolium chloride (TTC) staining**

| Group | Experimental procedure |
|---|---|
| Sham | Three days after surgery, the corresponding cortex was taken from three rats for miRNA array analysis, and from five rats for TTC staining |
| Cerebral ischemia/reperfusion injury | Three days after surgery, tissue around the lesion in ischemic ipsilateral cortex was taken from three rats for microRNA array analysis, and the whole brain from five rats for TTC staining |

**Table 2 Purity assessment of total RNA harvested from the ipsilateral cortex of ischemic rats using a Nanodrop spectrophotometer**

| Sample ID | OD260/280 ratio | OD260/230 ratio | Conc. (ng/μL) | Volume (μL) | Quantity (ng) | Quantity control result |
|---|---|---|---|---|---|---|
| Cerebral ischemia/ reperfusion injury | 2.00 | 2.24 | 1,508.39 | 10 | 15,083.90 | Pass |
| Sham | 2.00 | 2.26 | 878.04 | 20 | 17,560.80 | Pass |

There was no indication that the total RNA was contaminated with protein or organic compounds, and instead the harvested sample is high-purity total RNA. OD: Optical density; Conc.: concentration.

2 minutes, and then hybridized to the microarray for 16–20 hours at 56°C in a 12-Bay Hybridization Systems (Hybridization System; Nimblegen Systems, Inc., Madison, WI, USA). Following hybridization, slides were washed several times using a Wash buffer kit (Exiqon), and dried by centrifugation for 5 minutes at 80 × *g*. Slides were then scanned using the Axon GenePix 4000B microarray scanner (Axon Instruments, Foster City, CA, USA).

Scanned images were imported into GenePix Pro 6.0 software (Axon) for grid alignment and data extraction. All microarray signals were analyzed by subtracting the background, and normalized using Median normalization. In all samples, only normalized intensity ratios > 2 or < 0.5 (fold change ≥ 2.0) were defined as significantly changed miRNAs and included in the calculation.

**Bioinformatic analysis of differentially expressed miRNAs**

According to both normalized intensities and fold changes of miRNAs identified by microarray, the top 10 up- and down-regulated differentially expressed miRNAs were selected, and their main functional categories analyzed using GO-Analysis, which is based on Gene Ontology (http://www.geneontology.org/). GO-Analysis covers three domains: biological process (BP), cellular component (CC), and molecular function (MF).

Next, miRNA-GO-Network was used to determine the core gene function centralized by multiple miRNAs. First, miRNA target genes were determined from prediction databases (miRecords, Targetscan, MicroCosm, Miranda, and Pictar), with the intersection of retrieval results from these databases selected. Using topGO analysis for target genes, enrichment results of significant BP in GO-analysis were obtained. Finally, miRNAs with enrichment results of BP via gene-sets association were connected, and miRNA-GO-Network mapping constructed. Overlap counts > 10 and overlap coefficients > 0.4 were used as a strength index for correlation. In the maps, red square-type nodes represents miRNAs, and blue black circular nodes represent function terms. Node size reflects how many edges correlated.

Furthermore, predicted target genes of differentially expressed miRNAs were also analyzed by pathway analysis: a functional analysis method that maps genes to Kyoto Encyclopedia of Genes and Genomes (KEGG) pathways. *P*-values indicate the significance of correlated pathways, with lower P-values indicating more significant pathways (recommended *P*-value cut-off is 0.05).

## Results

**Successful establishment of a rat model of cerebral ischemia/reperfusion injury**

We used TTC staining to demonstrate infarction and determine the infarct volume. Compared with the sham group, TTC dye stained a significant white infarct area in both the cortex and striatum in the cerebral ischemia/reperfusion injury group (**Figure 1A**), with the percentage of corrected infarct volume calculated as 29.08 ± 1.39 (**Figure 1B**). These results confirm that the rat MCAO model was successfully induced by intraluminal obstruction and reperfusion.

**Assessment of total RNA quality**

The ratio of 260 nm to 280 nm absorbance (OD260/280 ratio) in all samples was between 1.8 and 2.1, while the ratio of 260 nm to 230 nm absorbance (OD260/230 ratio) was > 1.8. There was no obvious indication that the total RNA was contaminated with protein or organic compounds (**Table 2**). Agarose gel electrophoresis demonstrated intense and clear 28S and 18S ribosomal RNA bands, with no obvious degradation (**Figure 2**). These results indicate high purity and integrity of the total RNA obtained, and suggests that our samples met the requirement for the subsequent miRNA microarray experiments.

**miRNA expression profiles in rat cortex following cerebral ischemia/reperfusion injury**

To identify the miRNA expression profile in rat cortex after focal cerebral ischemia/reperfusion injury, the 6th generation miRCURY™ LNA Array (v.16.0) (Exiqon), which contains more than 1,891 capture probes, was used to detect differentially expressed miRNAs. A signal strength (normalized intensity) ratio > 2 or < 0.5 was considered to indicate

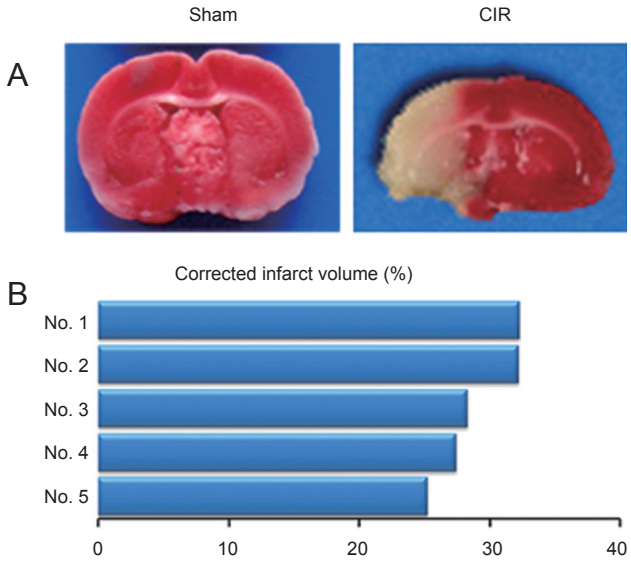


**Figure 1 Ischemic brain lesions in a rat model of cerebral ischemia/reperfusion injury (CIR).**
(A) Representative TTC-stained coronal brain slices show the infarct area as white and non-ischemic regions or healthy tissue as red. (B) Bars show the infarct volume for each rat in the CIR group ($n$ = 5). The corrected infarct volume was calculated as corrected infarct areas × section thickness (2.0 mm), and is expressed as a percentage of the contralateral hemisphere.

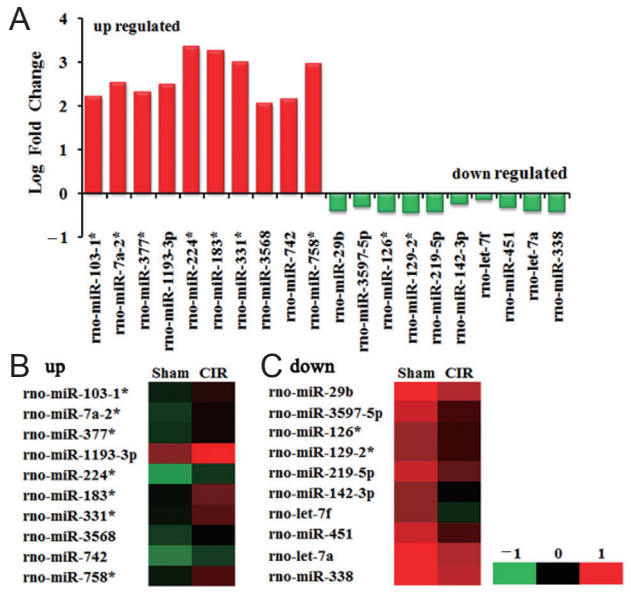


**Figure 3 Differentially expressed miRNAs detected by microarray in the cortex following cerebral ischemia and reperfusion injury.**
(A) The graph shows significantly changed miRNAs selected by fold change and normalized intensity. Bars above the abscissa represent the top 10 up-regulated miRNAs, while bars below the abscissa represent the top 10 down-regulated miRNAs. (B) Heat map of the top 10 up-regulated miRNAs. (C) Heat map of the top 10 down-regulated miRNAs. Heat maps were constructed using signal log ratio values, with up-regulated miRNAs shown in red and down-regulated miRNAs in green. The color column from green to red depicts altered miRNA expression from lowest to highest. CIR: Cerebral ischemia/reperfusion.

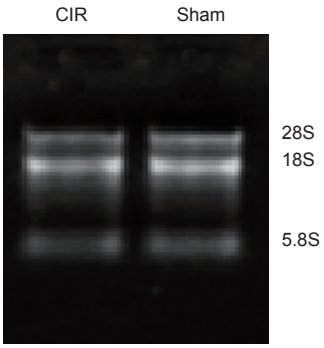


**Figure 2 Assessment of total RNA integrity by denaturing agarose gel electrophoresis.**
Agarose gel electrophoresis demonstrated distinct 28S and 18S ribosomal RNA bands, with no degradation bands. CIR: Cerebral ischemia/reperfusion.

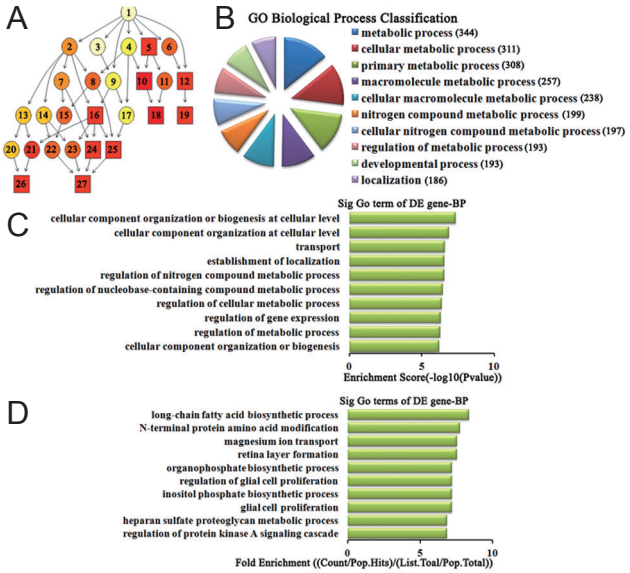


**Figure 4 Biological process classification in GO analysis of the top 10 up-regulated miRNAs.**
(A) The *P*-value tree structure illustrates the cascade relationship of each biological process regulated by the top 10 up-regulated miRNAs. 1: Biological process; 2: metabolic process; 3: biological regulation; 4: cellular process; 5: cellular component; 6: localization; 7: nitrogen compound metabolic process; 8: cellular metabolic process; 9: regulation of biological process; 10: cellular component organization or biogenesis at cellular level; 11: cellular component organization; 12: establishment of localization; 13: macromolecule metabolic process; 14: primary metabolic process; 15: cellular nitrogen compound metabolic process; 16: regulation of metabolic process; 17: regulation of cellular metabolic process; 18: cellular component organization at cellular level; 19: transport; 20: gene expression; 21: regulation of macromolecule metabolic process; 22: nucleobase-containing compound metabolic process; 23: regulation of primary metabolic process; 24: regulation of nitrogen compound metabolic process; 25: regulation of cellular metabolic process; 26: regulation of gene expression; 27: regulation of nucleobase-containing compound metabolic process. (B) The pie chart shows the top 10 significant enrichment terms represented by the biological process, with larger sectors representing more significant enrichment. The numbers in brackets indicate the number of genes associated with the biological process represented by each sector of the pie chart. (C) Bar plot ranking of the top 10 biological processes based on enrichment score. (D) Bar plot ranking of the top 10 biological process based on fold enrichment. GO-Analysis was performed based on Gene Ontology (http://www.geneontology.org/). GO: Gene Ontology; BP: biological process.

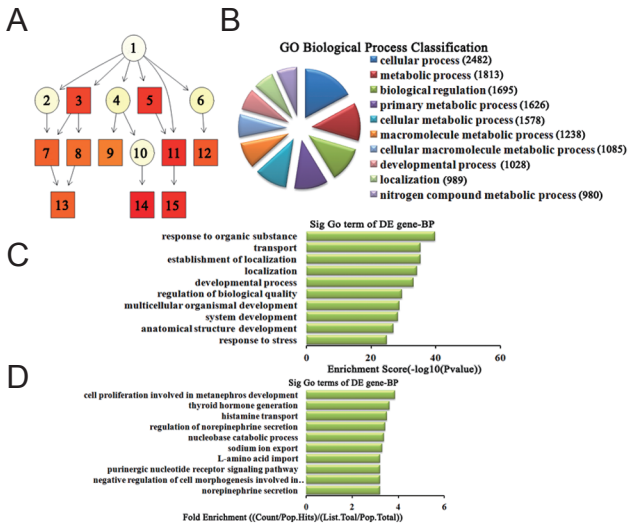


**Figure 5 Biological process classification in GO analysis of the top 10 down-regulated miRNAs.**
(A) The *P*-value tree structure illustrates the cascade relationship of each biological process regulated by the top 10 down-regulated miRNAs. 1: Biological process; 2: multicellular organismal development; 3: developmental process; 4: response to stimulus; 5: localization; 6: biological regulation; 7: multicellular organismal development; 8: anatomical structure development; 9: response to stress; 10: response to chemical substance; 11: establishment of localization; 12: regulation of biological quality; 13: system development; 14: response to organic substance; 15: transport. (B) The pie chart shows the top 10 significant enrichment terms represented by the biological process, with larger sectors representing more significant enrichment. The numbers in brackets indicate the number of genes associated with the biological process represented by each sector of the pie chart. (C) Bar plot ranking of the top 10 biological processes based on enrichment score. (D) Bar plot ranking of the top 10 biological processes based on fold enrichment. GO-Analysis was performed based on Gene Ontology (http://www.geneontology.org/). GO: Gene Ontology; BP: biological process.

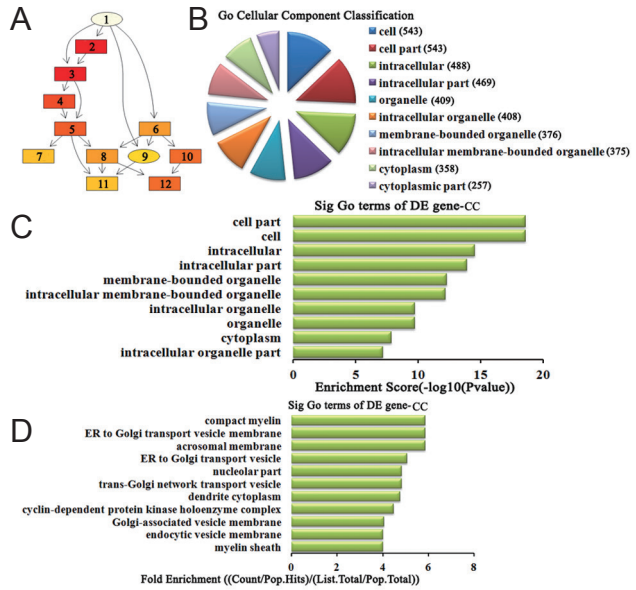


**Figure 6 Cellular component classification in GO analysis of the top 10 up-regulated miRNAs.**
(A) The *P*-value tree structure illustrates the cascade relationship between each cellular component and the top 10 up-regulated miRNAs. 1: Cellular component; 2: cell; 3: cell part; 4: intracellular; 5: intracellular part; 6: organelle; 7: cytoplasm; 8: intracellular organelle; 9: organelle part; 10: membrane-bounded organelle; 11: intracellular organelle part; 12: intracellular membrane-bounded organelle. (B) The pie chart shows the top 10 significant enrichment terms represented by the cellular component, with larger sectors representing more significant enrichment. The numbers in brackets indicate the number of genes associated with the cellular component represented by each sector of the pie chart. (C) Bar plot ranking of the top 10 cellular components based on enrichment score. (D) Bar plot ranking of the top 10 cellular components based on fold enrichment. GO-Analysis was performed based on Gene Ontology (http://www.geneontology.org/). GO: Gene Ontology; BP: biological process; CC: cellular component.

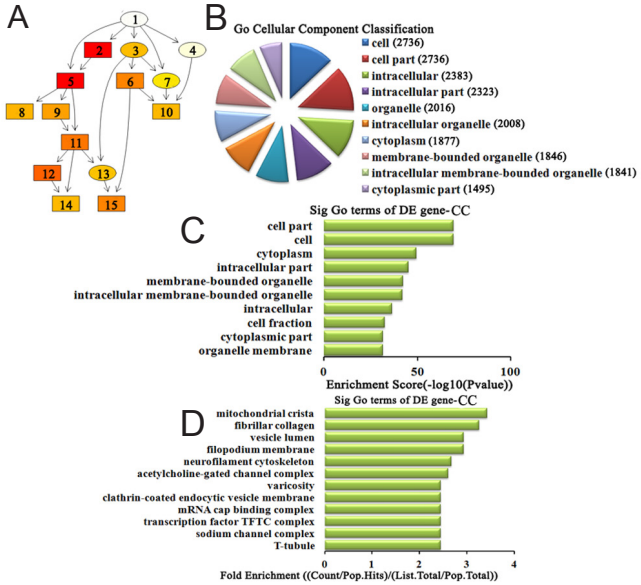


**Figure 7 Cellular component classification in GO analysis of the top 10 down-regulated miRNAs.**
(A) The *P*-value tree structure illustrates the cascade relationship between each cellular component and the top 10 down-regulated miRNAs. 1: Cellular component; 2: cell; 3: organelle; 4: membrane; 5: cell part; 6: membrane-bounded organelle; 7: organelle part; 8: cell fraction; 9: intracellular; 10: organelle membrane; 11: intracellular part; 12: cytoplasm; 13: intracellular organelle; 14: cytoplasmic part; 15: intracellular membrane-bounded organelle. (B) The pie chart shows the top 10 significant enrichment terms represented by cellular component, with larger sectors representing more significant enrichment. The numbers in brackets indicate the number of genes associated with the cellular component represented by each sector of the pie chart. (C) Bar plot ranking of the top 10 cellular components based on enrichment score. (D) Bar plot ranking of the top 10 cellular components based on fold enrichment. GO-Analysis was performed based on Gene Ontology (http://www.geneontology.org/). GO: Gene Ontology; CC: cellular component.

differentially expressed miRNAs using the fold change method. We identified a total of 15 miRNAs up-regulated and 44 miRNAs down-regulated, strikingly more than twice, in the cortex of rats with cerebral ischemia/reperfusion injury compared with rats in the sham group (**Table 2**). We selected the top 10 up- and down-regulated differentially expressed miRNAs for subsequent bioinformatics analysis, based on the largest quantitative value of both fold change and normalized intensity. Our selection of up-regulated miRNAs included rno-miR-224*, -183*, -331*, -758*, -7a-2*, -1193-3p, -377*, -103-1*, -742, and -3568, and of down-regulated miRNAs included rno-miR-338, -29b, -let-7a, -219-5p, -451, -3597-5p, -129-2*, -126*, -let-7f, -142-3p (**Figure 3**).

**Gene Ontology analysis of differentially expressed miRNAs**

Using GO-analysis, the functional categories associated with our top 10 up- and down-regulated miRNAs were determined, and found to cover three domains: biological process, cellular component, and molecular function.

*Biological process analysis of differentially expressed miRNAs*

For up-regulated miRNAs, the cascade relationship of each biological process can be seen from the *P*-value tree structure (**Figure 4A**). The most correlated biological processes were: metabolic process, cellular component organization or biogenesis at the cellular level, and long-chain fatty acid biosynthetic process, according to count (**Figure 4B**), enrichment score (**Figure 4C**), and fold enrichment (**Figure 4D**) of target gene GO terms. Similarly, for down-regulated miRNAs, the cascade relationship of each biological process is displayed in the P-value tree structure (**Figure 5A**). The most correlated biological processes were: cellular process, response to organic substance, and cell proliferation involved in metanephros development, according to count (**Figure 5B**), enrichment score (**Figure 5C**), and fold enrichment (**Figure 5D**) of target gene GO terms.

*Cellular component analysis of differentially expressed miRNAs*

For up-regulated miRNAs, the cascade relationship of each cellular component can be seen from the P-value tree structure (**Figure 6A**). The most related cellular components were: cell, cell part, and compact myelin, according to count (**Figure 6B**), enrichment score (**Figure 6C**), and fold enrichment (**Figure 6D**) of target gene GO terms. Similarly, for down-regulated miRNAs, the cascade relationship of each cellular component is displayed in the P-value tree structure (**Figure 7A**). The most correlated cellular components were: cell, cell part, and mitochondrial crista, according to count (**Figure 7B**), enrichment score (**Figure 7C**), and fold enrichment (**Figure 7D**) of target gene GO terms.

*Molecular function analysis of differentially expressed miRNAs*

For up-regulated miRNAs, the cascade relationship of each molecular function can be seen from the *P*-value tree structure (**Figure 8A**). The most related molecular function was: binding and channel inhibitor activity, according to count (**Figure 8B**), enrichment score (**Figure 8C**), and fold enrichment (**Figure 8D**) of target gene GO terms. Similarly, for down-regulated miRNAs, the cascade relationship of each molecular function is displayed in the *P*-value tree structure (**Figure 9A**). The most correlated molecular functions were: binding, protein binding, and L-glutamate transmembrane transporter activity, according to count (**Figure 9B**), enrichment score (**Figure 9C**), and fold enrichment (**Figure 9D**) of target gene GO terms.

**miRNA-GO-network analysis**

To identify the core gene function that is controlled intensively by multiple miRNAs, we constructed a miRNA-GO-network *via* gene-sets between miRNAs and significant biological processes using GO-analysis in Cytoscape software (http://www.Cytoscape.org). We found that metabolic process was the most concentrated biological process modulated by up-regulated miRNAs (**Figure 10**). In contrast, cellular process was centralized by down-regulated miRNAs (**Figure 11**). This suggests that multiple miRNAs co-participate and play key roles in regulating the same biological process.

**Pathway analysis of differentially expressed miRNAs**

To further study the functions and underlying mechanisms of these differentially expressed miRNAs under cerebral ischemia/reperfusion conditions, KEGG (http://www.genome.jp/kegg/) was used following GO analysis to examine the signaling pathways of specified miRNA target genes. We found that up-regulated miRNAs are involved in 30 pathways in the cerebral ischemia/reperfusion injury group compared with the sham group. According to enrichment score, D-glutamine and D-glutamate metabolism, and the renin-angiotensin system signaling pathway, are the main signaling pathways associated with up-regulated miRNAs (**Figure 12A**). The pathways most correlated with down-regulated miRNAs were peroxisome, peroxisome proliferator-activated receptor (PPAR) signaling pathway, SNARE interactions in vesicular transport, and calcium signaling pathway (**Figure 12B**).

## Discussion

Cerebral ischemia/reperfusion injury is a complex pathophysiological process, which is regulated by multiple factors. Recently, miRNAs were reported to act as important regulators in neuronal death induced by cerebral ischemia/reperfusion injury (Yu et al., 2015), suggesting that miRNAs may be responsible for cerebral ischemia/reperfusion injury. In this study, distinct patterns of miRNA expression following focal cerebral ischemia and reperfusion were detected by microarray analysis. A total of 15 miRNAs were up-regulated and 44 miRNAs down-regulated in the ipsilateral ischemic cortex of experimental rats. Among these, miR-29c targets both the *Birc2* and *Bak1* genes, and aggravates cerebral ischemia/reperfusion injury in rat models (Huang et al., 2015). Moreover, miR-21, miR-29b/c, miR-145, miR-181, miR-200 family, miR-338, and

miR let 7 family show altered expression levels in response to cerebral ischemia/reperfusion injury *in vivo* (Di et al., 2014). Another study also found that miR-21 and miR-29b are up-regulated in both neurons and astrocytes exposed to oxygen and glucose deprivation, which mimics ischemic conditions and reperfusion *in vitro* (Ziu et al., 2011). All of these miRNAs showing aberrant expression in cerebral ischemia/reperfusion were also detected in our microarray data. The remaining differentially expressed miRNAs in our microarray data have not yet been reported, and need to be further studied and validated. Until recently, most studies have focused on alterations in miRNA expression in the early stage of cerebral ischemia/reperfusion injury or the stage of most serious injury, but miRNA expression profiles and their roles during the middle and late stages of reperfusion have not been fully elucidated. Thus, we performed our study at the late phase of most serious injury.

MiRNAs are endogenous small noncoding RNA molecules that act as important regulators of target genes. In the central nervous system, miRNAs are correlated with the pathological processes of neurological diseases, including cerebral ischemia/reperfusion injury (Zhai et al., 2012). Increasing microarray studies of these miRNAs are currently available (Liu et al., 2013), but lack systematic analysis of the miRNAs biological functions and downstream signal transduction pathways. Therefore in this study, we selected the most dramatically changed miRNAs to perform further comprehensive bioinformatics analyses, including GO classification, miRNA-GO-network analysis, and KEGG pathway analysis. Our results indicate that up-regulated miRNAs are mainly involved in regulation of the metabolic process (**Figure 10**), while down-regulated miRNAs modulate the cellular process (**Figure 11**). The pathways associated with these functions are the renin-angiotensin system, D-glutamine and D-glutamate metabolism (**Figure 12A**), peroxisomes, the PPAR signaling pathway, SNARE interactions in vesicular transport, and the calcium signaling pathway (**Figure 12B**).

In the group of up-regulated miRNAs, metabolic process was at the center of the miRNA-GO-network (**Figure 10**), suggesting that the majority of up-regulated miRNAs co-participate and play a key role in the same biological process. It is well known that the brain exclusively depends on energy, and the energy supply-consumption balance must be maintained. Energy metabolic disorder is the basis of ischemic injury. Here, KEGG pathway analysis suggests that D-glutamine and D-glutamate metabolism signaling pathways are potentially implicated in the energy metabolic process. Glutamine is the main source of glutamate *via* enzymatic hydrolysis. Glutamate is the most abundant free amino acid in the brain (Furst et al., 1997), and is an important neurotransmitter of the central nervous system. During cerebral ischemia/reperfusion injury, disturbance of mitochondrial energy metabolism results in reduced ATP synthesis, triggering superfluous release of glutamate, increased additional influx of calcium, and aggravating cytotoxic edema and cellular injury (Hazell, 2007). Maintaining balance in glutamine and glutamate metabolism is a good strategy to eliminate the cellular damage from redundant glutamate. Our pathway analysis indicates that the renin-angiotensin system is also implicated in the ischemic metabolic process. The renin-angiotensin system is an important body fluid regulation system, and involved in regulation of the water-to-sodium metabolism to maintain fluid balance. Angiotensin II (Ang II) is the main active medium of the renin-angiotensin system, with its function implemented by the receptors $AT_1R$ and $AT_2R$. Following cerebral ischemia and reperfusion, Ang II and $AT_2R$ expression are significantly increased within brain tissue (Kagiyama et al., 2003), and persistently increased Ang II and $AT_1R$ may exacerbate cerebral edema and inflammatory damage (Schulz and Heusch, 2006). Research has shown that the brain renin-angiotensin system is involved in the pathological process of cerebral ischemia/reperfusion injury. Activation of the pro-inflammatory cytokine, nuclear factor-κB by Ang II may enhance the oxidative stress reaction and aggravate cerebral ischemia/reperfusion injury (Suzuki et al., 2003). This suggests that the up-regulated miRNAs are involved in metabolic processes associated with the renin-angiotensin system and D-glutamine and D-glutamate metabolism signaling pathways, and likely play a significant role in cerebral ischemia/reperfusion injury.

The majority of down-regulated miRNAs co-participated in regulation of the cellular process (**Figure 11**). Our pathway analysis results suggest that peroxisomes, the PPAR signaling pathway, SNARE interactions in vesicular transport, and the calcium signaling pathway correlate with regulation of this biological function *via* down-regulated miRNAs. Electron microscopy observations (Edinger and Thompson, 2004) have shown there are three types of cell death induced by cerebral ischemia and/or reperfusion: necrosis, apoptosis, and autophagy. Necrosis dominates the ischemic core, while apoptosis and autophagy mainly occupy the penumbra surrounding the ischemic core. Rami et al. (2008) found that autophagy and apoptosis might interact in the peri-infarct area after cerebral ischemia. Following cerebral ischemia and reperfusion, disordered energy metabolism leads to depolarization of mitochondrial membrane potentials, thereby generating excessive reactive oxygen species (ROS). When excess ROS generation overwhelms the capacity of endogenous free radical removal systems such as peroxisomes, peroxidation damage of lipids, proteins, nucleic acids, and polysaccharides subsequently occurs (Stadtman and Levine, 2000). Activation of PPARβ inhibits oxidative stress and the inflammatory response related to catalase up-regulation (Pesant et al., 2006). In the PPAR gene knockout mouse, expression levels of superoxide dismutase and glutathione were significantly decreased, while interferon-γ significantly increased (Arsenijevic et al., 2006). In addition to peroxidation damage, mitochondrial membrane potential depolarization triggers additional calcium influx (Kimelberg, 2005), the mitochondrial permeability transition pore opens (Fraser, 2011), cytochrome c is released (Ott et al., 2002) promoting the release of pro-apoptotic proteins (Kagan et al., 2005), and thereby initiating the cell death cascade. Moreover, the SNARE protein can regulate

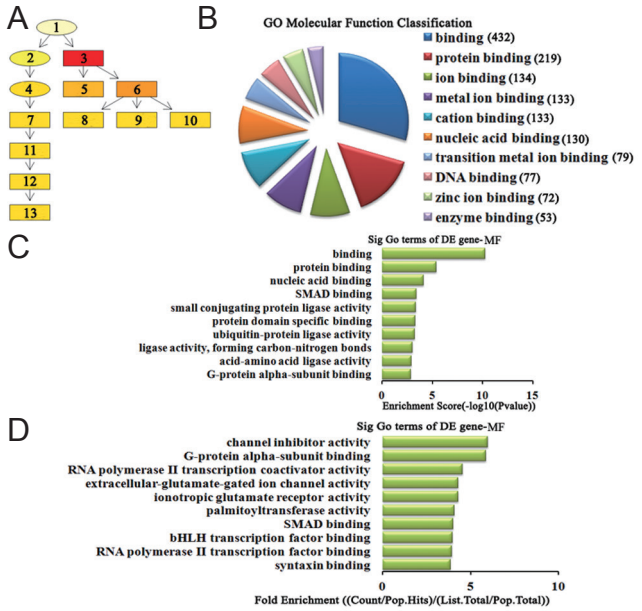


**Figure 8 Molecular function classification in GO analysis of the top ten up-regulated miRNAs.**

(A) The *P*-value tree structure illustrates the cascade relationship of each molecular function regulated by the top 10 up-regulated miRNAs. 1: Molecular function; 2: catalytic activity; 3: binding; 4: ligase activity; 5: nucleic acid binding; 6: protein binding; 7: ligase activity, forming carbon-nitrogen bounds; 8: G-protein alpha-subunit binding; 9: protein domain specific binding; 10: SMAD binding; 11: acid-amino acid ligase activity; 12: small conjugating protein ligase activity; 13: ubiquitin-protein ligase activity. (B) The pie chart shows the top 10 significant enrichment terms represented by molecular function, with larger sectors representing more significant enrichment. The numbers in brackets indicate the number of genes associated with the molecular function represented by each sector of the pie chart. (C) Bar plot ranking of the top 10 molecular functions based on enrichment score. (D) Bar plot ranking of the top 10 molecular functions based on fold enrichment. GO-Analysis was performed based on Gene Ontology (http://www.geneontology.org/). GO: Gene Ontology; MF: molecular function.

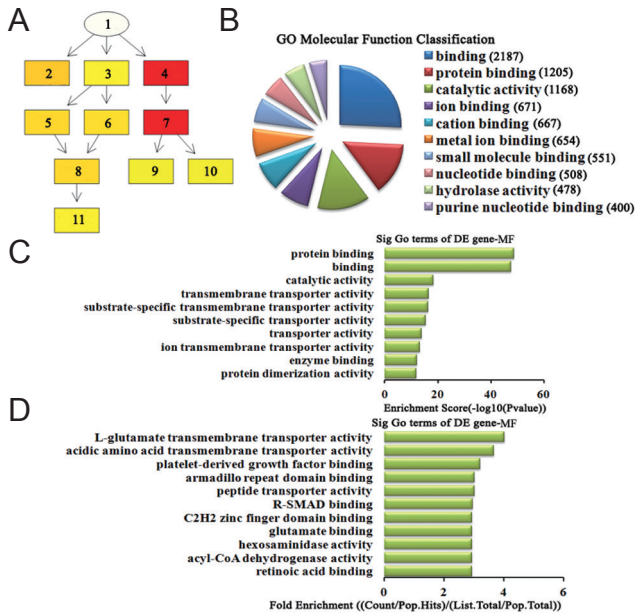


**Figure 9 Molecular function classification in GO analysis of the top ten down-regulated miRNAs.**

(A) The *P*-value tree structure illustrates the cascade relationship of each Molecular function regulated by the top 10 down-regulated miRNAs. 1: Molecular function; 2: catalytic activity; 3: transporter activity; 4: binding; 5: transmembrane transporter activity; 6: substrate-specific transporter activity; 7: protein binding; 8: substrate-specific transmembrane transporter activity; 9: enzyme binding; 10: protein dimerization activity; 11: ion transmembrane transporter activity. (B) The pie chart shows the top 10 significant enrichment terms represented by molecular function, with larger sectors representing more significant enrichment. The numbers in brackets indicate the number of genes associated with the molecular function represented by each sector of the pie chart. (C) Bar plot ranking of the top 10 molecular functions based on enrichment score. (D) Bar plot ranking of the top 10 molecular functions based on fold enrichment. GO-Analysis was performed based on Gene Ontology (http://www.geneontology.org/). GO: Gene Ontology; MF: molecular function.

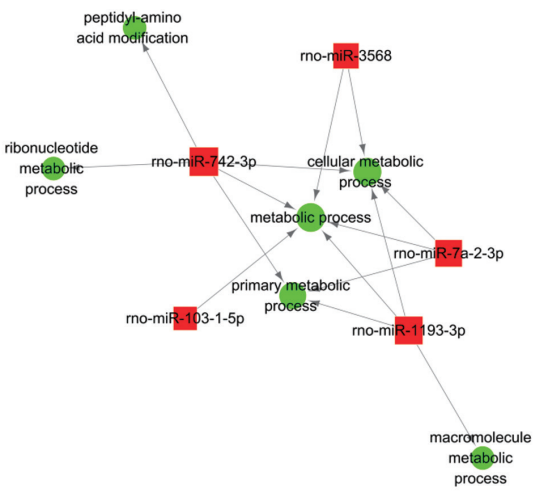


**Figure 10 miRNA-GO-network analysis *via* gene-sets of the top 10 up-regulated miRNAs.**

The network map reveals the core gene function controlled intensively by multiple miRNAs. Green marked nodes were associated with GO biological process analysis using Cytoscape software (http://www.cytoscape.org), and red marked nodes are associated with up-regulated miRNAs.

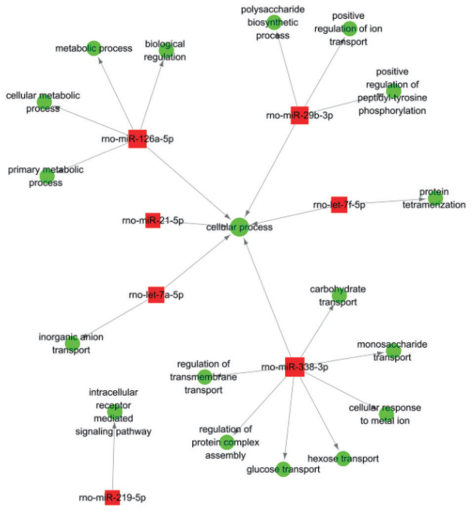


**Figure 11 miRNA-GO-network analysis *via* gene-sets of the top ten down-regulated miRNAs.**

The network map reveals the core gene function controlled intensively by multiple miRNAs. Green marked nodes represent GO biological process analysis in Cytoscape software (http://www.cytoscape.org), and red marked nodes represent down-regulated miRNAs.

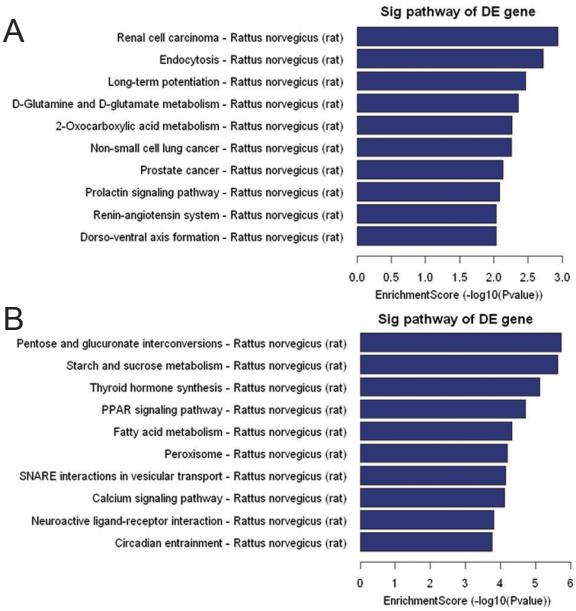


**Figure 12 KEGG pathway analysis associated with predicted target genes of the top 10 differentially expressed miRNAs.**
Following GO analysis, the Kyoto Encyclopedia of Genes and Genomes (KEGG) (http://www.genome.jp/kegg/) was used to analyze the signaling pathways of specified miRNA target genes. (A) Bar plot ranking of the top 10 enrichment score (–log10(*P*-value)) values for significant enrichment pathways of up-regulated miRNAs. (B) Bar plot ranking of the top 10 enrichment score (–log10(*P*-value)) values for significant enrichment pathways of down-regulated miRNAs.

all cell membrane fusion events because it is a key component of the cell membrane fusion protein complex (Kashiwada et al., 2009) and plays an important role in vesicular transport. In the nervous system, the SNARE complex mediates membrane fusion between neurotransmitter vesicles and the presynaptic membrane, releasing neurotransmitters, which are induced by calcium influx (Peters and Mayer, 1998). Upon reperfusion, disordered energy metabolism results in reduced ATP synthesis but increased ROS generation, triggering oxidative stress including the endoplasmic reticulum stress-autophagy response (Ron, 2001). Autophagy is a hydrolytic process mediated by lysosomes. Activation of autophagy after cerebral ischemia may be a protective mechanism because it clears cytotoxic substances but also eventually induces cell collapse and death if the autophagy is persistently activated (Rami et al., 2008). In the late stage of autophagy, autophagosome and lysosome fusion are typical vesicle fusion events mediated by the SNARE protein. These findings suggest that with cerebral ischemia/reperfusion injury, peroxisomes, the PPAR signaling pathway, SNARE interactions in vesicular transport, and the calcium signaling pathway are involved in cellular processes such as necrosis, apoptosis, and autophagy, and these processes are potentially modulated by the down-regulated miRNAs identified from our microarray data.

## Conclusion

MiRNA expression profiles are significantly changed in the reperfusion phrase of focal cerebral ischemia. To the best of our knowledge, we have systematically analyzed for the first time, the biological functions and downstream signaling pathways associated with target genes of miRNAs using bioinformatic prediction methods. The differentially expressed miRNAs were mainly involved in cellular metabolic processes and played an important role in infarction-related brain injury. Although our findings require further investigation, they suggest that miRNAs are likely to be a novel promising therapeutic target, and may shed light on the molecular mechanism of cerebral ischemia/reperfusion injury.

**Author contributions:** *XLM designed and performed the research, analyzed the data, and wrote the paper. TYW, YC, and JL analyzed and interpreted the data. JTL and THW provided critical revision of the paper. THW was responsible for fundraising, and designed and supervised the research. All authors approved the final version of this paper.*
**Conflicts of interest:** *None declared.*
**Plagiarism check:** *This paper was screened twice using Cross-Check to verify originality before publication.*
**Peer review:** *This paper was double-blinded, stringently reviewed by international expert reviewers.*

## References

Arai H, Passonneau JV, Lust WD (1986) Energy metabolism in delayed neuronal death of CA1 neurons of the hippocampus following transient ischemia in the gerbil. Metab Brain Dis 1:263-278.
Arsenijevic D, de Bilbao F, Plamondon J, Paradis E, Vallet P, Richard D, Langhans W, Giannakopoulos P (2006) Increased infarct size and lack of hyperphagic response after focal cerebral ischemia in peroxisome proliferator-activated receptor beta-deficient mice. J Cereb Blood Flow Metab 26:433-445.
Dharap A, Bowen K, Place R, Li LC, Vemuganti R (2009) Transient focal ischemia induces extensive temporal changes in rat cerebral microRNAome. J Cereb Blood Flow Metab 29:675-687.
Di Y, Lei Y, Yu F, Changfeng F, Song W, Xuming M (2014) MicroRNAs expression and function in cerebral ischemia reperfusion injury. J Mol Neurosci 53:242-250.
Edinger AL, Thompson CB (2004) Death by design: apoptosis, necrosis and autophagy. Curr Opin Cell Biol 16:663-669.
Fagan AM, Perrin RJ (2012) Upcoming candidate cerebrospinal fluid biomarkers of Alzheimer's disease. Biomark Med 6:455-476.
Fraser PA (2011) The role of free radical generation in increasing cerebrovascular permeability. Free Radic Biol Med 51:967-977.
Furst P, Pogan K, Stehle P (1997) Glutamine dipeptides in clinical nutrition. Nutrition 13:731-737.
Hazell AS (2007) Excitotoxic mechanisms in stroke: an update of concepts and treatment strategies. Neurochem Int 50:941-953.

Horn M, Schlote W (1992) Delayed neuronal death and delayed neuronal recovery in the human brain following global ischemia. Acta Neuropathol 85:79-87.
Huang LG, Li JP, Pang XM, Chen CY, Xiang HY, Feng LB, Su SY, Li SH, Zhang L, Liu JL (2015) MicroRNA-29c correlates with neuroprotection induced by FNS by targeting both Birc2 and Bak1 in rat brain after stroke. CNS Neurosci Ther 21:496-503.
Jeyaseelan K, Lim KY, Armugam A (2008) MicroRNA expression in the blood and brain of rats subjected to transient focal ischemia by middle cerebral artery occlusion. Stroke 39:959-966.
Jiang Y, Li L, Tan X, Liu B, Zhang Y, Li C (2015) miR-210 mediates vagus nerve stimulation-induced antioxidant stress and anti-apoptosis reactions following cerebral ischemia/reperfusion injury in rats. J Neurochem 134:173-181.
Kagan VE, Tyurin VA, Jiang J, Tyurina YY, Ritov VB, Amoscato AA, Osipov AN, Belikova NA, Kapralov AA, Kini V, Vlasova, II, Zhao Q, Zou M, Di P, Svistunenko DA, Kurnikov IV, Borisenko GG (2005) Cytochrome c acts as a cardiolipin oxygenase required for release of proapoptotic factors. Nat Chem Biol 1:223-232.
Kagiyama T, Kagiyama S, Phillips MI (2003) Expression of angiotensin type 1 and 2 receptors in brain after transient middle cerebral artery occlusion in rats. Regul Pept 110:241-247.
Kam KY, Yu SJ, Jeong N, Hong JH, Jalin AM, Lee S, Choi YW, Lee CK, Kang SG (2011) p-Hydroxybenzyl alcohol prevents brain injury and behavioral impairment by activating Nrf2, PDI, and neurotrophic factor genes in a rat model of brain ischemia. Mol Cells 31:209-215.
Kashiwada A, Tsuboi M, Matsuda K (2009) Target-selective vesicle fusion induced by molecular recognition on lipid bilayers. Chem Commun (Camb) (6):695-697.
Kimelberg HK (2005) Astrocytic swelling in cerebral ischemia as a possible cause of injury and target for therapy. Glia 50:389-397.
Lages E, Ipas H, Guttin A, Nesr H, Berger F, Issartel JP (2012) MicroRNAs: molecular features and role in cancer. Front Biosci (Landmark Ed) 17:2508-2540.
Lim KY, Chua JH, Tan JR, Swaminathan P, Sepramaniam S, Armugam A, Wong PT, Jeyaseelan K (2010) MicroRNAs in cerebral ischemia. Transl Stroke Res 1:287-303.
Liu DZ, Tian Y, Ander BP, Xu H, Stamova BS, Zhan X, Turner RJ, Jickling G, Sharp FR (2010) Brain and blood microRNA expression profiling of ischemic stroke, intracerebral hemorrhage, and kainate seizures. J Cereb Blood Flow Metab 30:92-101.
Liu FJ, Lim KY, Kaur P, Sepramaniam S, Armugam A, Wong PT, Jeyaseelan K (2013) microRNAs involved in regulating spontaneous recovery in embolic stroke model. PLoS One 8:e66393.
Longa EZ, Weinstein PR, Carlson S, Cummins R (1989) Reversible middle cerebral artery occlusion without craniectomy in rats. Stroke 20:84-91.
Lust WD, Taylor C, Pundik S, Selman WR, Ratcheson RA (2002) Ischemic cell death: dynamics of delayed secondary energy failure during reperfusion following focal ischemia. Metab Brain Dis 17:113-121.
Ott M, Robertson JD, Gogvadze V, Zhivotovsky B, Orrenius S (2002) Cytochrome c release from mitochondria proceeds by a two-step process. Proc Natl Acad Sci U S A 99:1259-1263.
Pesant M, Sueur S, Dutartre P, Tallandier M, Grimaldi PA, Rochette L, Connat JL (2006) Peroxisome proliferator-activated receptor delta (PPARdelta) activation protects H9c2 cardiomyoblasts from oxidative stress-induced apoptosis. Cardiovasc Res 69:440-449.
Peters C, Mayer A (1998) Ca2+/calmodulin signals the completion of docking and triggers a late step of vacuole fusion. Nature 396:575-580.
Rami A, Langhagen A, Steiger S (2008) Focal cerebral ischemia induces upregulation of Beclin 1 and autophagy-like cell death. Neurobiol Dis 29:132-141.
Ron D (2001) Hyperhomocysteinemia and function of the endoplasmic reticulum. J Clin Invest 107:1221-1222.
Schulz R, Heusch G (2006) Angiotensin II type 1 receptors in cerebral ischaemia-reperfusion: initiation of inflammation. J Hypertens Suppl 24:S123-129.
Selvamani A, Sathyan P, Miranda RC, Sohrabji F (2012) An antagomir to microRNA Let7f promotes neuroprotection in an ischemic stroke model. PLoS One 7:e32662.
Sims NR, Muyderman H (2010) Mitochondria, oxidative metabolism and cell death in stroke. Biochim Biophys Acta 1802:80-91.
Stadtman ER, Levine RL (2000) Protein oxidation. Ann N Y Acad Sci 899:191-208.
Sun J, Tong L, Luan Q, Deng J, Li Y, Li Z, Dong H, Xiong L (2012) Protective effect of delayed remote limb ischemic postconditioning: role of mitochondrial K(ATP) channels in a rat model of focal cerebral ischemic reperfusion injury. J Cereb Blood Flow Metab 32:851-859.
Suzuki Y, Ruiz-Ortega M, Lorenzo O, Ruperez M, Esteban V, Egido J (2003) Inflammation and angiotensin II. Int J Biochem Cell Biol 35:881-900.
Tan KS, Armugam A, Sepramaniam S, Lim KY, Setyowati KD, Wang CW, Jeyaseelan K (2009) Expression profile of MicroRNAs in young stroke patients. PLoS One 4:e7689.
Wechsler LR (2011) Intravenous thrombolytic therapy for acute ischemic stroke. N Engl J Med 364:2138-2146.
Wu T, Ding XS, Wang W, Wu J (2006) MCI-186 (3-methyl-1-phenyl-2-pyrazolin-5-one) attenuated simulated ischemia/reperfusion injury in cultured rat hippocampal cells. Biol Pharm Bull 29:1613-1617.
Yellon DM, Hausenloy DJ (2007) Myocardial reperfusion injury. N Engl J Med 357:1121-1135.
Yu H, Wu M, Zhao P, Huang Y, Wang W, Yin W (2015) Neuroprotective effects of viral overexpression of microRNA-22 in rat and cell models of cerebral ischemia-reperfusion injury. J Cell Biochem 116:233-241.
Yuan Y, Wang JY, Xu LY, Cai R, Chen Z, Luo BY (2010) MicroRNA expression changes in the hippocampi of rats subjected to global ischemia. J Clin Neurosci 17:774-778.
Zhai F, Zhang X, Guan Y, Yang X, Li Y, Song G, Guan L (2012) Expression profiles of microRNAs after focal cerebral ischemia/reperfusion injury in rats. Neural Regen Res 7:917-923.
Ziu M, Fletcher L, Rana S, Jimenez DF, Digicaylioglu M (2011) Temporal differences in microRNA expression patterns in astrocytes and neurons after ischemic injury. PLoS One 6:e14724.

*Copyedited by James R, Raye W, Li CH, Song LP, Zhao M*